ACI STRUCTURAL JOURNAL TECHNICAL PAPER

Title no. 95-S38

Design of Slender Reinforced Concrete Walls with Openings

by Christopher P. Taylor, Paul A. Cote, and John W. Wallace

This paper summarizes the results of an experimental and analytical study of slender reinforced concrete structural walls with an opening at the base. The primary objectives of this research were the evaluation of a displacement-based approach for the selection of transverse boundary reinforcement, and the evaluation of a strut and tie model for the selection of the horizontal shear reinforcement. Two approximately quarter-scale wall specimens were constructed and tested under constant axial stress and reverse cyclic lateral loading.

Experimental results show that, when designed using a combined displacement-based and strut and tie approach, slender structural walls with openings at the base exhibit stable hysteretic behavior and significant ductility. The displacement-based design technique allowed transverse boundary reinforcement to be provided as needed rather than selected based on a nominal value. The strut and tie model was found to be an effective tool for the design of discontinuous regions, where simplified code equations are not appropriate.

Keywords: capacity design; displacement-based design; earthquake loads; flexural response; inelastic design; moment-curvature response; openings; plane-sections; reversed cyclic loads; shear deformations; shear walls; structural walls; strut and tie modeling; truss modeling; wall discontinuities; walls; walls with openings.

INTRODUCTION

The use of reinforced concrete structural walls is common for resisting lateral forces imposed by wind or earthquakes. In areas of high seismic risk, it is usually not feasible to design a structural wall to remain elastic during a severe earthquake;[1] therefore, inelastic deformations are expected, usually at the wall base. Allowing inelastic deformations reduces the force that the wall must resist, provides a "fuse" to limit damage to other elements in the structure, and can provide significant damping. In order to exhibit stable, inelastic behavior, the wall must be specially detailed; that is, transverse reinforcement must be provided in regions of high strain.

Current codes (e.g., UBC-94) include provisions for the design of symmetric and unsymmetric solid walls; however, it is often necessary to provide openings in the walls for doors or windows. If the openings are small relative to the wall dimensions, it may be reasonable to neglect the effects of the opening. However, in some cases, the opening is relatively large or is located in a critical region where inelastic deformations are expected. In such cases, the influence of the opening on the wall behavior must be evaluated.

Current U.S. codes do not provide adequate design guidelines for walls with openings; therefore, considerable judgment is required to evaluate the wall behavior. In general, the influence of the opening on the flexural and shear strength, as well as detailing requirements, should be considered. If the opening is near the middle of the wall, it will decrease the moment capacity of the wall only slightly; however, the shear strength may be significantly reduced. In contrast, an opening near a wall boundary may impact both shear and flexural strengths, depending on the size of the opening.

Relatively little testing has been done to evaluate the performance of walls with openings. Tests by Ali and Wight[2] on approximately one-quarter scale slender walls with staggered openings revealed the walls were vulnerable to shear compression failure when the opening at the base was located close to the wall boundary. Due to the scale of the specimens it was difficult to provide the staggered openings without locating the openings close to the wall boundary. For full-scale walls, they suggested that the use of walls with staggered openings was a viable option provided openings were not located too close to the wall boundary. One specimen was tested without openings, and excellent behavior to large drift ratios was observed even though the only moderate detailing of the boundary zones was provided compared with ACI 318-95 requirements. This behavior can be explained using a displacement-based design approach.[3] Tests by Yanez et al.[4] on stout walls designed using strut and tie models and capacity design indicated that pierced walls can exhibit significant ductility. The studies by Yanez el al.[4] suggest that a strut and tie approach may also be a robust tool for evaluation of slender walls with openings, such as those tested by Ali and Wight.[2]

ACI Structural Journal, V. 95, No. 4, July-August 1998.

Received January 27, 1997, and reviewed under Institute publication policies.
 Pertinent discussion will be published in the May-June 1999 *ACI Structural Journal* if received by January 1, 1999.

Christopher P. Taylor is an engineer-in-training with J. Muller International bridge design consultants, Chicago. He received his BS degree from the University of Maine at Orono in May 1994 and a MS degree from the Department of Civil and Environmental Engineering at Clarkson University in Potsdam, New York, in May 1996. This work was completed in partial fulfillment of his MS degree requirements at Clarkson University.

Paul A. Cote is a staff engineer at Spiegel Zamecnik and Shah, Inc. in New Haven, Connecticut. He received his BS and MS degrees from the Department of Civil and Environmental Engineering at Clarkson University in Potsdam, New York.

John W. Wallace is an associate professor of civil engineering at the University of California, Los Angeles. His research and teaching interests include behavior and performance of reinforced concrete structures subjected to earthquake loads, as well as field and laboratory testing. He has done extensive research on the behavior and design of reinforced concrete walls. He is a member of ACI Committees 318-H, 352, 368, and 369, and currently serves as the Chair of ACI Committee 368, Earthquake Resisting Systems and Elements.

Recently published research on the behavior of slender walls has shown that a displacement-based design approach provides a versatile design methodology.[3] Experimental studies have been conducted to validate the approach for walls with rectangular and T-shaped cross sections.[5] However, there is a need to evaluate the applicability of displacement-based design to walls with openings. In addition, the influence of the opening on the shear strength of the wall must be assessed.

RESEARCH SIGNIFICANCE

The focus of the current study is the design of slender reinforced structural walls with openings at the base, where inelastic deformations are concentrated. The proposed design procedure involves combining displacement-based design and strut and tie concepts. The design is broken down into a series of steps in which each type of reinforcement is selected. First, boundary longitudinal reinforcement is selected based on code prescribed forces and a standard cross sectional analysis, assuming plane sections remain plane. Second, the transverse reinforcement is selected using the displacement-based design procedure presented by Wallace[3] and verified experimentally for solid walls by Thomsen and Wallace.[5] Finally, the horizontal shear reinforcement is selected using capacity design and strut and tie models. The objective of this research is to experimentally verify that the use of a displacement-based design procedure and a strut and tie model with capacity design principles are appropriate for evaluating detailing and shear requirements of slender walls with relatively large openings at the base of the wall.

EXPERIMENTAL PROGRAM

Specimen description

Two one-quarter scale specimens were constructed, one with a rectangular cross section (RW3-O) and one with a barbell shaped (BW1-O) cross section. Materials used were 4000 psi (27.6 MPa) concrete and GR 60 (414 MPa) steel. Relatively large openings were provided at the base of each wall near the boundary. The wall geometries were selected to be similar to those tested by Thomsen and Wallace[5] and Ali and Wight;[2] therefore, direct comparison may be made between walls with and without openings. Detailing requirements were assessed using a displacement-based design approach for a design drift level of 1.5 percent. This drift level was used to be consistent with the value used by Thomsen and Wallace.[5]

The walls were 12 ft (3.66 m) high and 4 ft (1.22 m) long, resulting in an aspect ratio of 3. Each wall contained confined boundary regions. Elevation views of the walls showing the horizontal and vertical reinforcing details are shown in Fig. 1 and 3. Figures 2 and 4 show the cross sections of each wall at various levels. The following two sections contain detailed descriptions of the reinforcing provided for each wall.

Specimen RW3-O—The geometry for Specimen RW3-O was selected such that the results could be easily compared with those of Specimen RW2 tested by Thomsen and Wallace.[5] The walls tested by Thomsen and Wallace were roughly based on a six-story prototype building in an area of high seismic risk.

Overall dimensions and boundary longitudinal reinforcing were identical for Specimens RW3-O and RW2. The cross sections were 48 in. (1.22 m) long by 4 in. (102 mm) wide. Longitudinal reinforcement consisted of eight No. 3 (9.5 mm) deformed bars (Grade 60; 414 MPa) in each boundary. Longitudinal steel was continuous over the height of the wall and was anchored into a base pedestal with 90 deg hooks. The opening in specimen RW3-O, located adjacent to the south boundary region (see Fig. 5), was 12 in. (305 mm) wide by 27 in. (686 mm) high.

Transverse boundary reinforcing and web reinforcing for RW3-O varied from that provided for RW2 due to increased compressive strains at the wall boundaries and the interruption of shear flow within the web due to the opening. Transverse boundary reinforcement consisted of closed hoops and cross ties at a spacing of 2 in. (51 mm). The hoops and cross ties were fabricated from $^3/_{16}$ in. (4.8 mm) diameter smooth wire annealed to have stress-strain properties similar to U.S. Grade 60 reinforcement.[5] Up to 55 in. (1.40 m) above the base, a hoop and two cross ties were provided in the boundary adjacent to the opening; a hoop and one cross tie were provided at the other boundary. Above 55 in. (1.40 m), U-shaped hoops were lapped with the horizontal web steel at a spacing of 7.5 in. (191 mm).

Uniformly distributed vertical web steel consisted of two curtains of No. 2 (6.4 mm) deformed bars (Grade 60; 414 MPa) spaced at 7.5 in. (191 mm) over stories two and three. The spacing was reduced to 5 in. (127 mm) over the first story due to a concentration of shear stress caused by the opening. Also, adjacent to the opening, the two No. 2 (6.4 mm) bars were replaced with two No. 3 (9.5 mm) bars.

Distributed horizontal web steel also consisted of two curtains of No. 2 (6.4 mm) bars. The bars were spaced at 5 in. (127 mm) over the bottom 25 in. (635 mm), 3.75 in. (95 mm) over the next 15 in. (381 mm) (over the top of the opening), and 7.5 in. (191 mm) up to the fourth story. The horizontal ties over the bottom 55 in. were anchored into the confined boundary region using 90 deg hooks around a longitudinal bar. Both horizontal and vertical distributed web steel were doubled over the top story to account for potential stress concentrations due to load transfer.

Specimen BW1-O—The geometry for Specimen BW1-O was selected such that the results could be easily compared with those found for Specimens W1 and W2 (Ali and Wight,

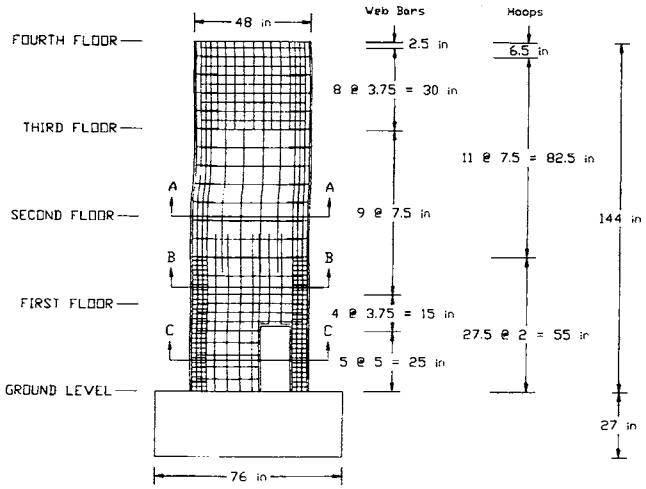

Fig. 1—RW3-O: Elevation view showing reinforcing

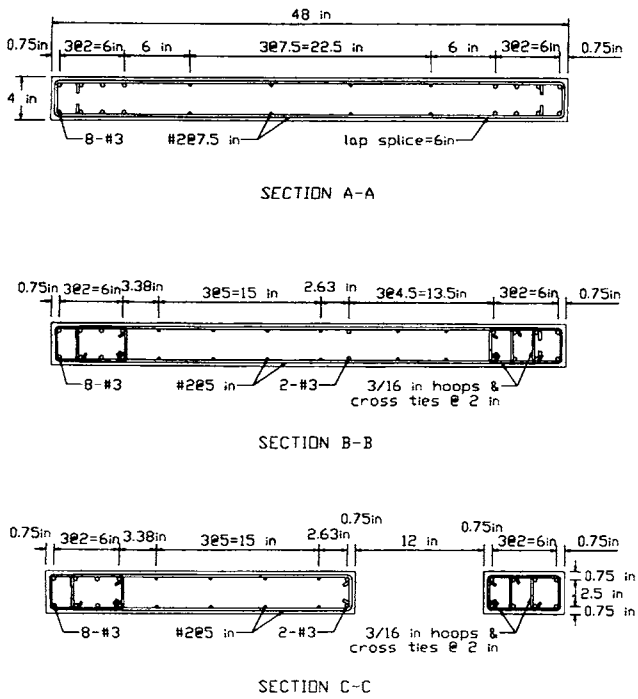

Fig. 2—RW3-O: Cross sections

1990), which were designed to be representative of walls used in Chilean construction. All three wall specimens had 5 × 5 in. (127 × 127 mm) boundary elements with a 38 × 3 in. (965 × 76 mm) web. Specimen W1 contained no openings, whereas W2 and BW1-O contained openings 9 in. (229 mm) wide by 20 in. (508 mm) high, located 3.5 in. (89 mm) from the edge of the wall. Specimen W2 contained openings staggered at each story; however, an opening only at the base was provided for BW1-O since this was the location of concentrated inelastic deformation. Longitudinal reinforcement consisted of four No. 4 (13 mm) deformed bars (Grade 60; 414 MPa) in each boundary. This resulted in approximately the same area of main longitudinal steel for both Specimens RW3-O (eight No. 3; 9.5 mm) and BW1-O (four No. 4; 13 mm).

For Specimen BW1-O, closed hoops were spaced at 3 in. (76 mm) in each boundary up to a height of 42 in. (1.07 m).

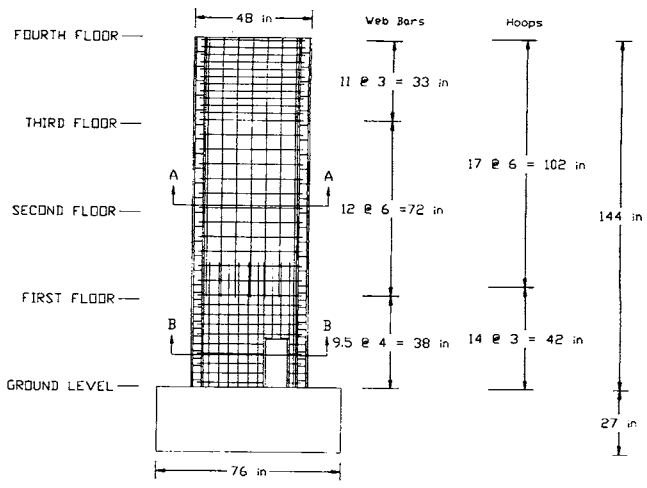

Fig. 3—BW1-O: Elevation view showing reinforcing

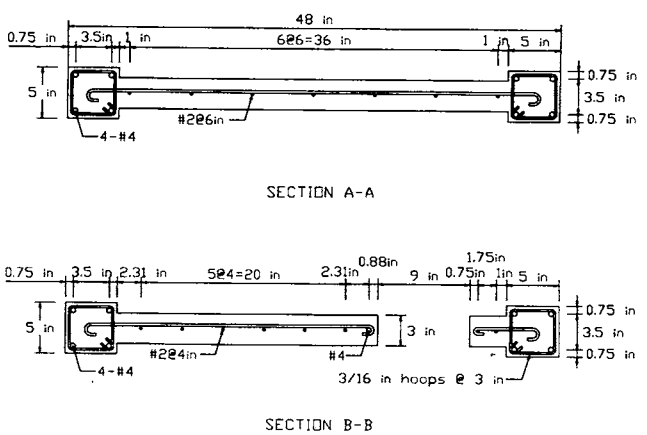

Fig. 4—BW1-O: Cross sections

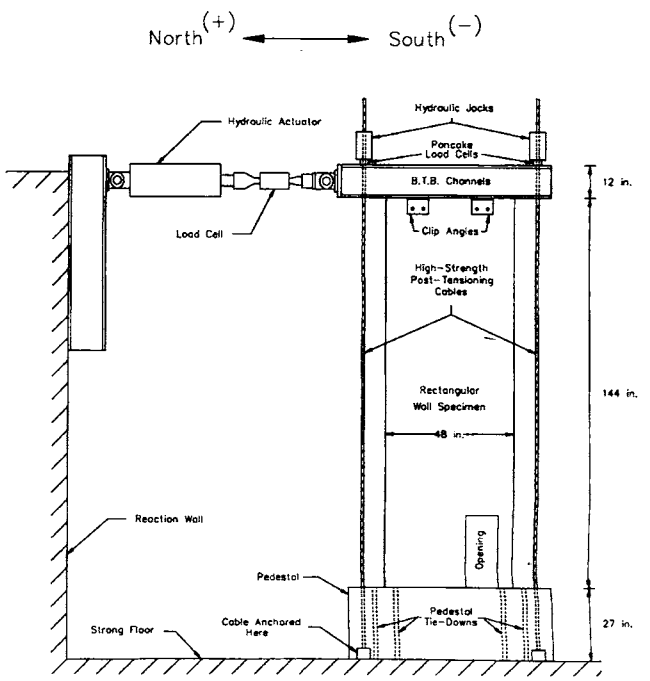

Fig. 5—Test setup

This spacing was selected based on a design drift level of 1.5 percent. Above 42 in. (1.07 m), the spacing of the hoops was increased to 6 in. (152 mm). Uniformly distributed vertical web steel consisted of a single curtain of No. 2 (6.4 mm) bars at 6 in. (152 mm) for the upper stories and 4 in. (102 mm) for the first story. The bar adjacent to the opening in the longer wall web section was replaced with a No. 4 (13 mm) bar. Horizontal web steel was also a single curtain of No. 2 (6.4 mm) bars, except over the opening, where four of the bars were replaced with No. 3 (9.5 mm) bars. The bars were spaced at 4 in. (102 mm) over the bottom 38 in. (965 mm), 6 in. (76 mm) over the next 72 in. (1.83 m), and 3 in. (76 mm) over the remainder of the wall. The horizontal ties were anchored in the boundary elements using 180 degree hooks. The closer spacing of the web steel around the opening of BW1-O as compared with W1 and W2 (Ali and Wight[2]) was based on the results of a strut and tie design, as is discussed later.

Material properties

Stress versus strain diagrams for the reinforcement used in the study are presented in Taylor and Wallace[9] and Thomsen and Wallace.[5] A standard ready mix with $^3/_8$ in. (9.5 mm) maximum aggregate was used. Concrete cylinder strengths at 28 days and at test date were 4000 (27.6 MPa) and 4500 (31.0 MPa), respectively, for both RW3-O and BW1-O. Representative concrete and steel stress-strain diagrams are presented by Thomsen and Wallace,[5] and are fairly typical for these materials.

Testing apparatus

The testing apparatus is shown in Fig. 5. Each specimen was attached to the strong floor using four $1^1/_4$ in. (32 mm) diameter rods at each end. A 150 kip (667 kN) hydraulic actuator attached to the reaction wall was used to apply a horizontal force to the load transfer assembly mounted on top of the wall. To ensure out of plane stability, a steel frame was attached between the top assembly and the reaction wall parallel to the specimen. At the reaction wall, the frame was free to slide in the direction parallel to the applied load. Axial load was provided with two hollow core hydraulic jacks on top of the load transfer assembly. Prestressing strands were anchored into the pedestal at the base of the wall and connected to jacks at the top of the wall. The jacks were controlled with a hand hydraulic pump to maintain constant axial load during the test. Additional testing information is available in Thomsen and Wallace[5] and Taylor and Wallace.[9]

Instrumentation and data acquisition

Instrumentation was provided to measure loads, displacements, and strains at critical locations. Lateral load was measured with a load cell placed between the actuator and the load transfer assembly. Axial loads were measured with hollow core load cells placed between the top chucks and the jacks (Fig. 5).

The horizontal displacement profile of each specimen was measured using wire potentiometers at each story level (at the base of the wall and at four locations over the wall height). The wire potentiometers were mounted on a steel reference frame connected independently to the strong floor. Linear potentiometers were provided at each end of the pedestal to determine the vertical displacement of the pedestal, from which the pedestal rotation was calculated. To obtain the rotation at the base of the wall, wire potentiometers were mounted at the first story height and connected to the pedestal to measure the vertical displacement of each side of the wall. Shear deformations were measured using wire potentiometers mounted in "X" configurations over each of the bottom two stories.

Longitudinal strains were measured three ways. First, steel strain gages were attached to reinforcing bars just above the base of the wall and at 36 in. (914 mm) and 28 in. (711 mm) above the base for specimens RW3-O and BW1-O, respectively. Second, concrete strain gages were embedded at various locations along the base of the wall. Finally, linear voltage differential transducers (LVDTs) were used to measure vertical displacement along the base of the wall over a gage length of approximately 9 in. (229 mm). Steel strain gages were also provided on numerous hoops and cross ties within the boundary regions and on horizontal reinforcement within the web.

Testing procedure

A axial load of approximately $0.10f'_cA_g$ was applied to the walls at the beginning of each test and held constant for the duration of each test. This level of axial load was used to represent a typical moderate-rise building. Load cells were used to monitor the axial load and minor adjustments were made with hand pumps during the test to maintain a constant axial load. Additional details are provided in the reports by Thomsen and Wallace[5] and Taylor and Wallace.[9] During each test, the displacement at the top of the wall was controlled. A reverse cyclic loading was applied slowly to the top of the specimens. Due to the likelihood that the wall would eventually fail when being pushed (southward displacement), each cycle began with pulling (northward displacement). Typically, two complete cycles were performed at each drift level. The drift levels investigated were approximately 0.10, 0.25, 0.50, 0.75, 1.0, 1.5, 2.0, 2.5, and 3.0 percent.

WALL DESIGN AND ANALYTICAL MODELING

Summary of design procedure

The overall dimensions and main longitudinal reinforcement were determined by flexural design to resist code earthquake forces on a scaled prototype wall used by Thomsen and Wallace.[5] For a design earthquake, the top story lateral drift demand was estimated and related to the curvature demand at the base of the wall using simplified equations. Using a sectional analysis, the required amount of transverse reinforcement could be selected such that the wall would not degrade excessively before reaching the curvature demand. Finally, a strut and tie model was developed to select horizontal shear reinforcement to ensure that horizontal force had an adequate load path to the base of the wall for the shear force that developed at wall flexural capacity. Details of each design step are provided in the following sections.

Flexural strength requirements

Longitudinal boundary reinforcement for Specimens RW3-O and BW1-O was selected to be identical to that used

in Specimen RW2, tested by Thomsen and Wallace,[5] and Specimens W1 and W2, tested by Ali and Wight,[2] respectively. The transverse reinforcement required at the wall boundaries for concrete confinement and to restrain buckling of the main longitudinal bars was selected using a displacement-based design technique. To ensure adequate wall deformability, a *moment-curvature* analysis incorporating the effect of the opening was used.

Displacement-based design

Wallace[3,6] presents a displacement-based design procedure for the seismic design of reinforced concrete shear walls. The procedure involves comparing the strain capacity of the wall with the estimated strains imposed on the wall as a result of a design earthquake. In general, the strain capacity of a wall can be increased by providing additional transverse boundary reinforcement. Thus, rather than providing an arbitrary amount of confining reinforcement at the wall boundaries, confinement is selected based on the deformation or strain demand.

Thomsen and Wallace[5] used a drift level of 1.5 percent since it provided a reasonable drift level to study detailing requirements at wall boundaries. The tests by Ali and Wight[2] on staggered walls, not designed using a displacement-based design approach, exhibited shear-compression failures at 1.5 percent drift level. A horizontal drift level of 1.5 percent was also used in this study to allow direct comparison with the study by Thomsen and Wallace,[5] and to evaluate the potential to improve on the behavior observed by Ali and Wight.[2] Roughly, a drift level of 1.5 percent corresponds to a displacement ductility of 2 to 3, since slender walls with moderate axial loads typically yield at 0.5 to 0.75 percent drift level. Once the imposed drift was determined, the curvature demand could then be related to the roof displacement demand using Eq. (1). Assuming a plastic hinge length of $l_w/2$ and a yield curvature of $0.0025/l_w$, the term $\phi_u l_w$ may be approximated as:[1]

$$\phi_u l_w = 0.0025\left[1 - \frac{1}{2}\frac{h_w}{l_w}\right] + 2\frac{\delta_u}{h_w} \qquad (1)$$

The first term accounts for elastic curvature over the height of the wall and the second term accounts for concentrated inelastic curvature in the base of the wall. Eq. (1) leads to a design curvature times wall length, $\phi_u l_w$, of 0.029, corresponding to a curvature of 0.00060 rad/in. (0.024 rad/m) for the 48 in. (1.22 m) wall specimens.

Moment-curvature analyses were conducted to determine the required amount of transverse reinforcement. A linear strain distribution was assumed with nonlinear material relations to model the stress distribution and the effects of concrete confinement. An iterative process was used to select the amount of confining steel at the wall boundaries such that the walls would not experience significant loss of strength at the design curvature. The resulting design strain distributions are shown in Fig. 6. The spacing of the $^3/_{16}$ in. (4.7 mm) diameter hoops was chosen as 2 in. (51 mm) and 3 in. (76 mm) for RW3-O and BW1-O, respectively. The spacings selected for concrete confinement were found to be adequate to prevent buckling of the main longitudinal bars.[4] The flexural compression zone extended beyond the opening for RW3-O and was approximately equal to the boundary column length for BW1-O (Fig. 6).

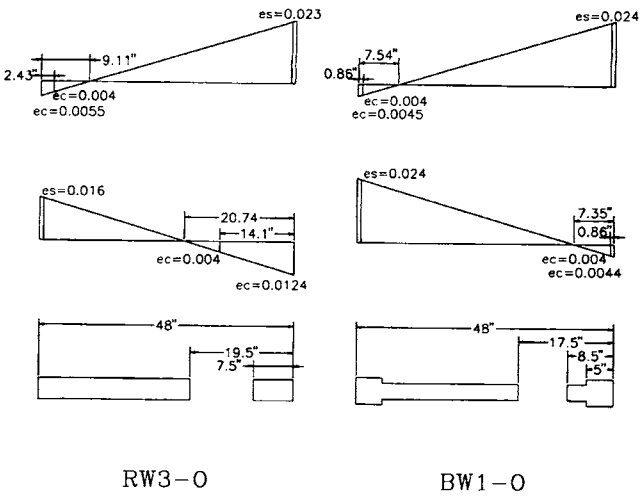

Fig. 6—Design strain profiles

Shear strength requirements

The shear design for the walls was evaluated independently from the flexural design. Due to the opening at the base of the wall, simplified code equations based on a uniform shear stress distribution over the wall cross section are not appropriate. To address this problem, selection of web reinforcement to provide shear resistance was based on use of a strut and tie model to ensure that an adequate load path was provided for the shear that would develop at the wall flexural capacity.

To ensure that shear failure would not control the behavior of the specimens and that the nominal flexural strength of the wall would be achieved, the horizontal design load at the top of the wall that was used for the strut and tie model was computed as the nominal flexural strength at the base of the wall divided by the wall height. Strain hardening and overstrength of the longitudinal reinforcement were considered in the evaluation of the flexural strength. The strut and tie models selected and the equilibrium forces are shown in Fig. 7 and 8. The models consisted of only struts, fans, ties, and nodes; shear friction, dowel action, and concrete arches were not used. Consistent with common U.S. practice, only orthogonal steel was used. A model with overlapping ties spaced at 12 in. (305 mm) was selected. Use of a 12-in. (305 mm) model tie spacing only affects the fineness of the model and does not determine the spacing of the actual ties.

The axial load was accounted for by applying one-half of the load to the top of each chord of the truss. The horizontal load was applied as a single point load at the top of the wall; although a uniform load across the top of the wall is more realistic. The actual load application at the top of the wall is of little significance since the region of interest is at the base of the wall.

Based on the results of finite element analysis, Sittipunt and Wood[8] suggest that diagonal reinforcement around the opening is most effective in improving the inelastic behavior

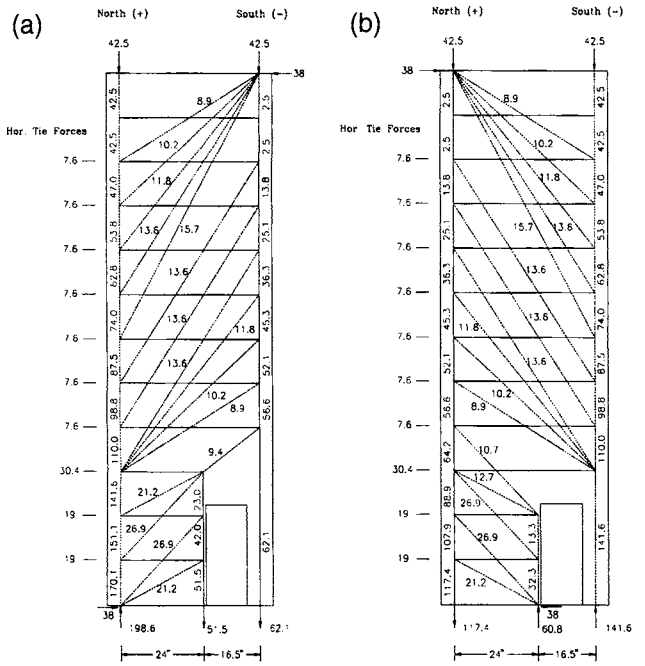

Fig. 7—RW3-O: Strut and tie models, positive and negative directions (load in kips)

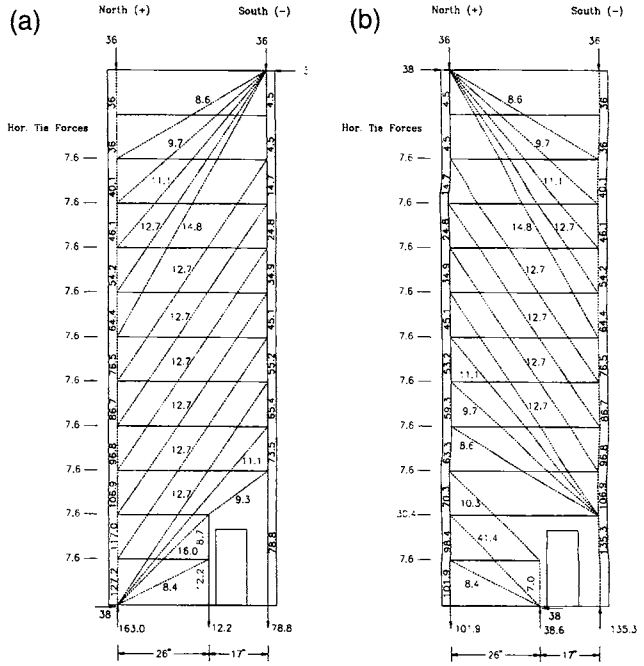

Fig. 8—BW1-O: Strut and tie models, positive and negative directions (load in kips)

of walls with openings. In the test specimens, however, consistent with common U.S. construction practice, a mesh of vertical and horizontal reinforcement was used in place of diagonal reinforcement. Although the strut and tie models that were idealized do not require vertical web reinforcement, it was provided at the same spacing as the horizontal web reinforcement to provide a uniform mesh that is similar to that provided by diagonal reinforcement, as well as to control crack widths.

EXPERIMENTAL RESULTS

A summary of experimental results of the two wall specimens tested are presented in the following sections. Additional information is available in Taylor and Wallace.[9] In addition to comparing the results for the two walls tested in this study, comparisons are made with walls tested by Thomsen and Wallace[5] and Ali and Wight.[2] The experimental results discussed include: 1) observed damage and behavior; 2) lateral load versus top displacement relations; 3) base moment versus first story rotation relations; 4) lateral displacement profiles; 5) shear distortion relations; and 6) strain profiles at the wall base.

Observed behavior and load-displacement response

Figures 9 and 10 show the applied lateral load versus top displacement relations for Specimens RW3-O and BW1-O, respectively. The applied lateral load was measured using a load cell mounted between the hydraulic actuator and the top loading assembly. Top displacement was measured using a wire potentiometer. For both RW3-O and BW1-O, the point of yielding can be identified to occur at approximately 0.75 percent drift in both directions of loading. It can also be seen in the figures that the stiffness in the positive direction is only slightly greater than in the negative direction for each specimen. Detailed descriptions of the observed behavior and measured load-displacement response are discussed in the following paragraphs.

RW3-O—Yielding of the main longitudinal bars occurred during the cycle to 0.75 percent lateral drift. At 1.5 percent drift, spalling began on the north end of the wall and also became more pronounced at the column (smaller portion of the wall at the south boundary). Spalling also began on the inside face of the column at the top of the opening. After two cycles at 1.5 percent drift, two additional cycles at 1.0 percent were completed, during which very little additional damage occurred. Two additional cycles at 1.5 percent resulted in a very slight increase in crack lengths and spalling. The first cycle at 2.0 percent caused significant spalling on the north boundary and most of the concrete cover on the column had split and was loose. This cover concrete fell off during the second cycle, primarily along a diagonal from the bottom outside edge of the column to the top inside edge of the column. A third cycle was performed at 2.0 percent drift. During the only cycle at 2.5 percent drift, the column began to buckle out of plane and the applied horizontal load began to decrease, indicating impending failure. Since the north boundary was still intact, testing in this direction was continued. When approaching 3.0 percent drift, the northern main longitudinal bars buckled and the boundary element concrete crushed.

The behavior of RW3-O is compared with that for specimen RW2 tested by Thomsen and Wallace.[5] The major differences in the walls (RW2 and RW3-O) include: (1) the opening in RW3-O, which affected the distribution of the web reinforcing; (2) intermediate cross ties were provided within the south boundary element of RW3-O due to the high compressive strains (Fig. 6); (3) the average axial load for Specimen RW2 was $0.07A_g f'_c$ compared with $0.099A_g f'_c$ for RW3-O. The overall behavior of the walls was very similar, and was dominated by flexural yielding at the base. The load

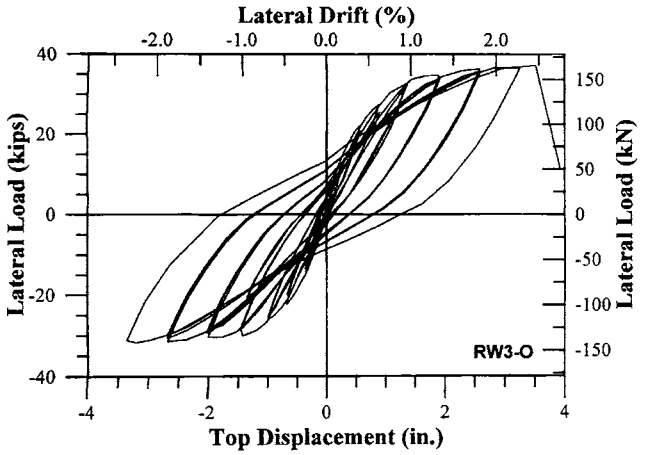

Fig. 9—RW3-O: Lateral load vs. top displacement

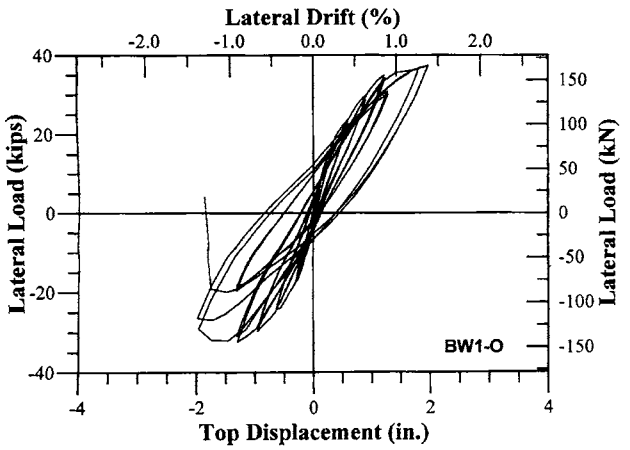

Fig. 10—BW1-O: Lateral load vs. top displacement

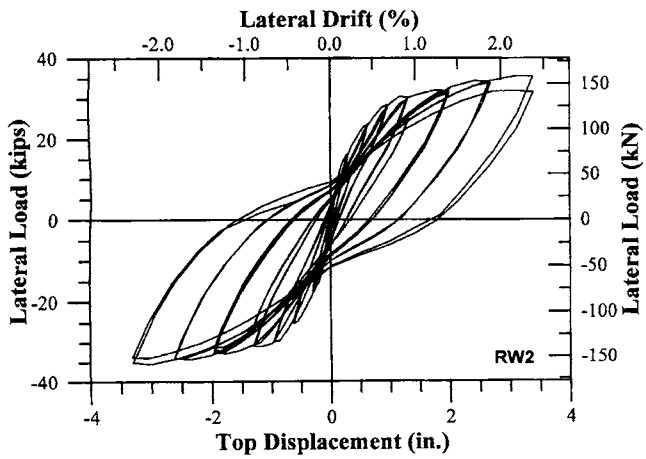

Fig. 11—RW2: Lateral load vs. top displacement[5]

versus top displacement relation of RW3-O (Fig. 9) was very similar to Specimen RW2 (Fig. 11), except for a slight reduction in strength when the column was in compression. Both walls exhibited stable behavior to about 2.5 percent drift and reached approximately the same peak load. The longitudinal bars in Specimen RW2 buckled after three cycles at 2.5 percent drift, in a similar manner to those in the north boundary of RW3-O.

BW1-O—Overall load-displacement response is presented in Fig. 10. At 0.75 percent drift, the longitudinal bars in Specimen BW1-O also began to yield. During the second half of the first cycle at 1.0 percent drift, spalling started on the outside of the column, approximately 5 in. (127 mm) from the base. During the repeat cycle, spalling began on the top inside of the column and vertical splitting occurred in the narrow web section between the opening and the boundary element. This section of the web crushed and the No. 2 (6.4 mm) longitudinal bars buckled during the first cycle at 1.5 percent drift. During the second cycle, one of the main longitudinal bars at the outside corner buckled and the small web section had deteriorated to the point where it was no longer effective in resisting load. Buckling of the main bar at this stage was influenced by an improperly spaced hoop. This hoop was offset 0.5 in. (13 mm) on one corner, resulting in a spacing of 3.5 in. (89 mm). Two additional cycles at 1.0 percent drift showed a reduced strength but continued stable behavior. During the second half of the third cycle at 1.5 percent, the concrete within the column boundary element crushed and the remaining bars in the boundary buckled. Had the hoops been spaced correctly it is anticipated that Specimen BW1-O would have exhibited stable behavior to a higher drift level.

Specimen BW1-O had the same gross geometry as Specimens W1 (solid) and W2 (openings) tested by Ali and Wight.[2] The main differences between specimens BW1-O and W2 were: 1) the spacing of the transverse hoops within the boundary, 3 in. (76 mm) in BW1-O versus 2.5 in. (64 mm) in W1 and W2; 2) BW1-O did not have diagonal reinforcing at the corners of the opening; 3) BW1-O had an opening only at the base and not staggered openings in the upper stories; and 4) BW1-O had more web steel, which was selected based on a strut and tie. Specimen W1 was nearly the same as W2 except it contained no openings. An axial load of $0.07A_g f'_c$ was applied to W1 and W2 whereas $0.137A_g f'_c$ was applied to BW1-O. Both Specimens BW1-O and W2 experienced shear compression failure in the narrow pier during the third cycles at 1.5 percent drift, while W1 failed during the first cycle at 3.0 percent drift. Although one of the main longitudinal bars in BW1-O buckled prematurely, it still performed similarly to Specimen W2, which had more tightly spaced hoops and lower axial stress. The results indicate the difficulties associated with the use of a single curtain of web reinforcement and the importance of proper placement of hoops and cross ties at the wall boundary. As well, by comparison of the results for Specimens W1, W2, and BW1-O, it is apparent that openings can have a significant impact on wall deformation capacity and failure modes and that this influence must be accounted for in design.

Base moment versus first story rotation relations

Base moment versus first story rotation relations are plotted in Fig. 12 and 13 for Specimens RW3-O and BW1-O, respectively. The base moment was calculated as the applied lateral load times the height of the load application above the base (150 in.; 3.81 m). The first story rotation was calculated as the difference in the displacements measured with wire

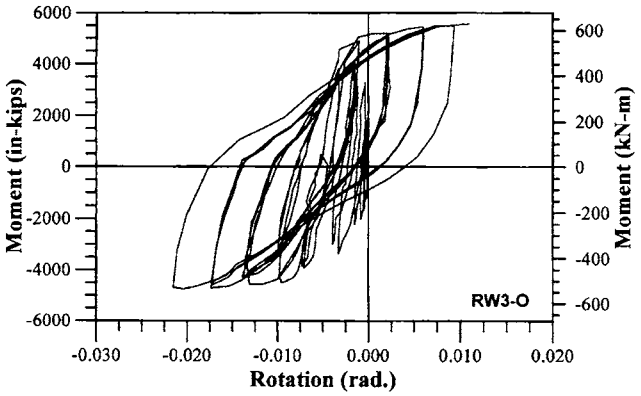

Fig. 12—RW3-O: Base moment vs. first-story rotation

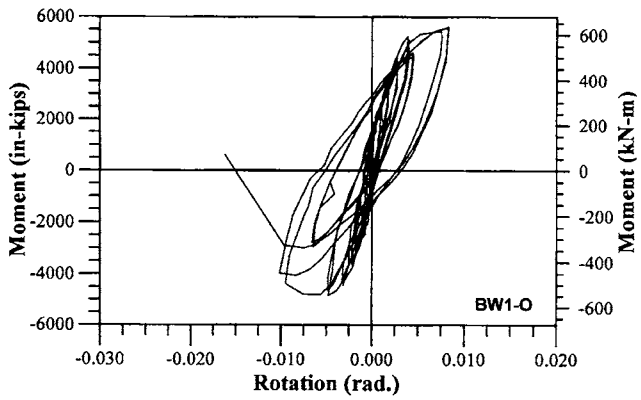

Fig. 13—BW1-O: Base moment vs. first-story rotation

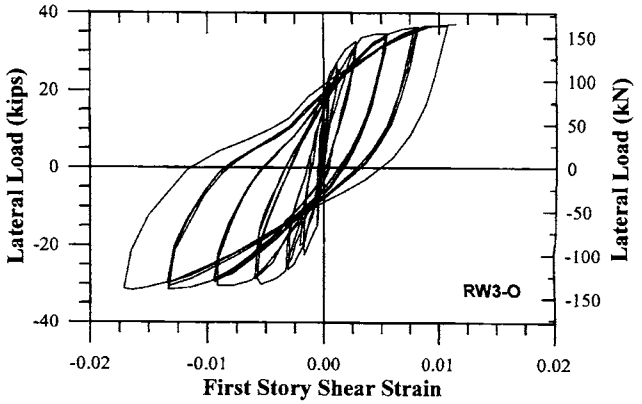

Fig. 14—RW3-O: Average shear strain over first story

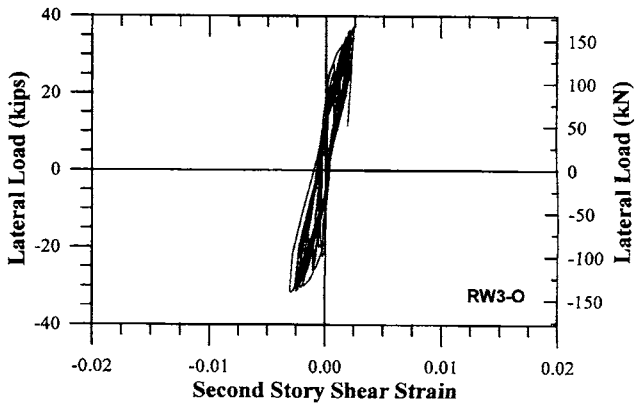

Fig.15—RW3-O: Average shear strain over second story

potentiometers, located 30 in. (762 mm) above the base on each side of the wall, divided by the distance between the potentiometers. The flexural strength, calculated for the actual material properties, is also shown on Fig. 12 and 13. The full loops shown in Fig. 12 indicate that RW3-O had good energy absorption capability. Due to the presence of the opening, the peak moment is slightly less and the first story rotation is approximately twice as large when the specimen is subjected to negative load (column in compression). The larger inelastic deformations in the negative direction cause the loops to progressively shift in the negative direction. The curve in Fig. 13 shows that Specimen BW1-O exhibited stable behavior to only 0.01 radians.

Shear distortion relations

Average shear strain for the first and second stories of RW3-O are shown in Fig. 14 and 15. Shear distortions were measured using wire potentiometers in an "X" configuration as described earlier. The average shear strain over each story was calculated as:

$$\gamma_{ave} = \frac{(d'_1 - d_1)d_1 - (d'_2 - d_2)d_2}{2hl} \quad (2)$$

where d_1 and d_2 are the undeformed lengths of the wire potentiometers, d'_1 and d'_2 are the deformed lengths, and h and l are the height and length of the "X" configuration.

When the column was in compression, RW3-O experienced approximately 1.5 times the first story shear deformation that RW2 experienced, although the horizontal applied load was nearly the same. When the column was in tension, the deformations in RW3-O were only slightly greater. Specimens RW3-O, BW1-O, and RW2 all showed that the shear deformations in the second story were relatively small, varied little with the direction of loading, and were approximately the same for each wall.

Components of top displacement

The contribution of pedestal rotation and shear deformations to top displacement are shown in Fig. 16. The pedestal rotation component was calculated as the pedestal rotation times the sum of the wall height and the pedestal height (144 and 27 in.; 3.66 and 0.69 m). Pedestal rotation accounted for up to 15 percent of the top displacement for each wall. The shear component was calculated as the measured average shear strain times the story height. Shear deformations were only measured over the first two stories. The third and fourth story shear deformations were assumed to be the same as for the second story, since the shear force is constant and large flexural cracks were limited to the bottom story. At 1.5 percent drift, the shear component was 20 and 28 percent of the top displacement for RW3-O under positive and negative loading, respectively. These are significantly higher than RW2,[5] in which shear accounted for only 10 percent of the top displacement. The results show that shear deformations

were greater when the columns were in compression (wall section at south boundary), even though the shear force was slightly less. Thomsen and Wallace[5] found the component of top displacement due to steel slip at the base to be insignificant; therefore, the flexural component is taken as the measured top displacement minus the shear and pedestal rotation components.

Strain profiles at the base of the walls

Reinforcing steel strain gages—Figures 17 and 18 show the steel strain profiles across the base of Specimen RW3-O. The strain profiles for Specimen BW1-O were very similar. These figures indicate that up to 0.75 percent drift, which is when the outermost longitudinal steel began to yield, the strain profile across the section was very nearly linear. Beyond 0.75 percent drift, the strain profile became significantly nonlinear. As was found by Ali and Wight,[2] the two panels on either side of the opening acted somewhat independently indicating that it may not be appropriate to connect the strain profile across the opening with a straight line. Figures 17 and 18 show that, at 1.0 percent drift, strain relaxation began to occur in Specimen RW3-O due to bond deterioration. Specimen BW1-O did not show significant strain relaxation at this drift level.

LVDTs—The strain profiles at the base of the wall as calculated from the LVDTs for RW3-O in each direction are shown in Fig. 19 and 20. Strains were calculated by dividing the displacement recorded from the LVDTs by the gage length of approximately 9 in. (223 mm). Since this is an average strain over the gage length, the LVDTs show much less variation than the steel strain gages. As was seen with the longitudinal steel strain profiles, above approximately 0.75 percent drift, the strain profiles became noticeably nonlinear. Since the displacement history applied to the wall consisted of north displacement (column tension) followed by south displacement (column compression), a direct comparison of the design strain distributions determined from a monotonic analysis and experimentally measured strain distributions is not as useful as it would be if the testing were conducted by first placing the column in compression. Since the evaluation of the strain distribution across the opening was one of the objectives of this study, use of this modified testing routine may have been more useful. Alternatively, a moment-curvature analysis that accounts for cyclic response could be used to allow direct comparison of results. Comparisons of measured responses for RW2 and RW3-O are made later in this paper to assess the impact of cyclic loads.

Figures 17 through 20 show that there was increased curvature within the column, as compared to the north panel, both in tension and in compression. Thus, it may not be appropriate to assume that this panel is a uniaxially loaded column as could be assumed for design. Specimens RW2 (Thomsen and Wallace[5]) and W1 (Ali and Wight[1]), which had no openings, exhibited fairly linear strain distribution at the base. Strain profiles for W2, which did have openings, exhibited similar trends in nonlinear behavior as observed for RW3-O and BW1-O. As suggested by Ali and Wight,[2] the nonlinear strain distributions in Specimens RW3-O, BW1-O, and W2 indicate that it may not be appropriate to assume a linear strain distribution across the opening. The impact of this result on wall design is assessed later in this paper.

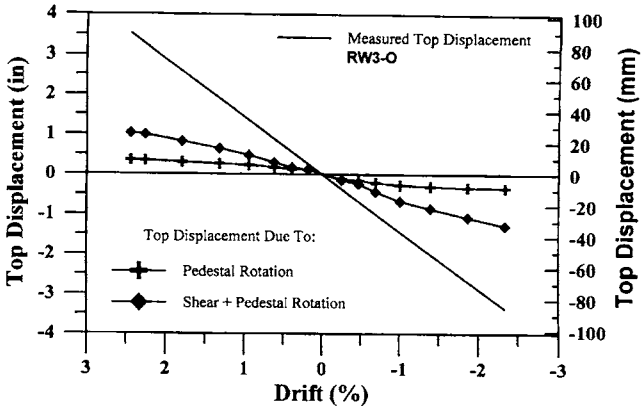

Fig. 16—RW3-O: Components of top displacement

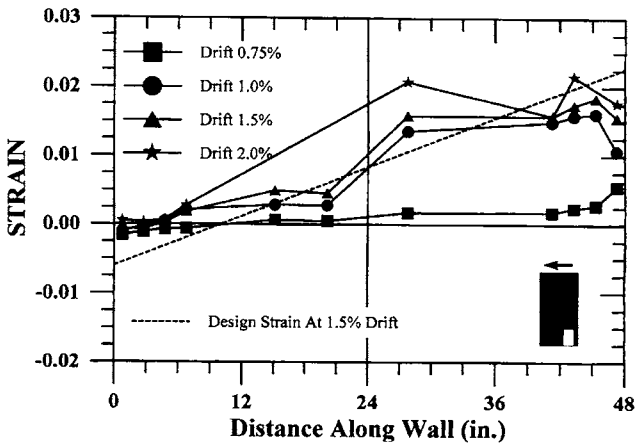

Fig. 17—RW3-O: Analytical vs. measured steel strain profiles (positive displacement)

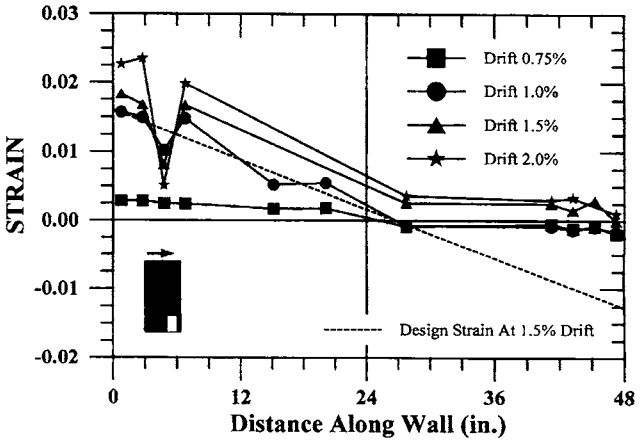

Fig. 18—RW3-O: Analytical vs. measured steel strain profiles (negative displacement)

DISCUSSION OF RESULTS

This section presents a comparison between the experimentally observed and the analytically predicted results. The

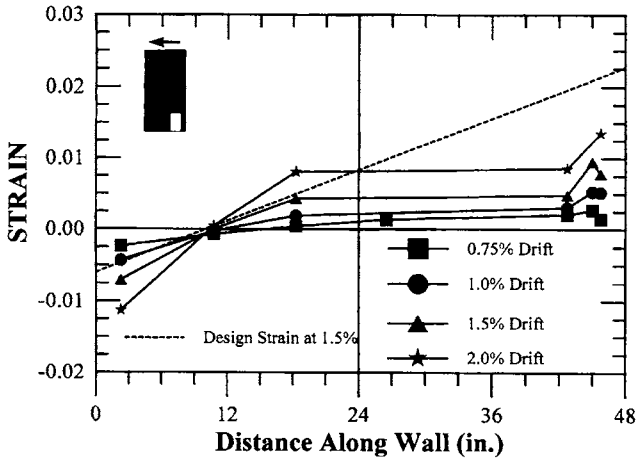

Fig. 19—RW3-O: Analytical vs. measured concrete strain profiles (positive displacement)

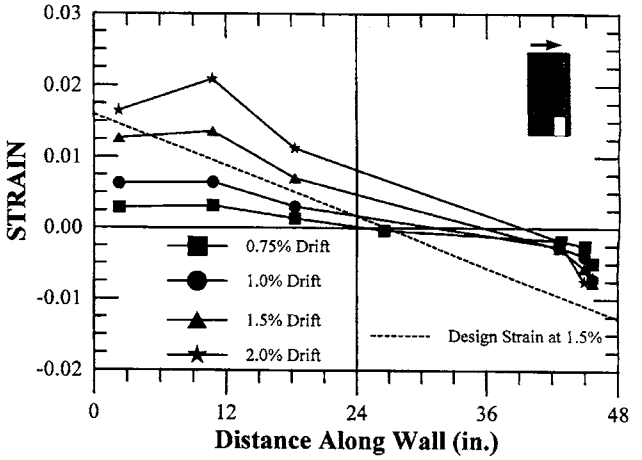

Fig. 20—RW3-O: Analytical vs. measured concrete strain profiles (negative displacement)

following are investigated: 1) normal strain distributions; 2) moment-curvature relations; and 3) strut and tie load paths.

Strain distributions

The assumed strain distributions at the wall base at 1.5 percent drift are compared to those measured experimentally with the steel strain gages and with the LVDTs in Fig. 17 through 20 for RW3-O. Figures 17 and 18 reveal that, for Specimen RW3-O, the design strain distributions predicted the measured steel tensile strain distributions well; however, the actual compressive strain in the column was significantly less than predicted. This is attributed to inelastic deformation in tension causing the steel to carry compressive stress before it returned to zero strain. An analysis that accounts for cyclic loads might be helpful; however, this level of detail may not be practical for design, which is the focus of this paper. The steel strain distributions for BW1-O show similar behavior, although the actual strains were not as high as predicted, especially when the column was in tension.

The LVDTs indicate that the design strains for Specimen RW3-O predict the concrete strains well (Fig. 19 and 20); however, the comparison was not as close as those for solid rectangular and T-shaped walls tested by Thomsen and Wallace[5] (Fig. 26). When the column was in tension (Fig. 19), the actual concrete strains were about 50 percent greater than expected, possibly due to the influence of shear, since the compression struts for loading in this direction converge at the wall boundary (Fig. 7).

Overall, the linear strain distributions used for design agree with the measured strains reasonably well; however, since the column and the wall panel could act somewhat independently, local variation in the strains is expected. The linear strain distribution assumed for design allowed for the selection of transverse reinforcement, which performed well. Since the column at the wall boundary plays a critical role in the overall performance, a conservative quantity of transverse reinforcement should be provided. For a narrow web section adjacent to confined boundary zone, additional transverse reinforcement should be provided, or the performance of the wall should be assessed assuming that this section may become ineffective, as occurred for Specimen BW1-O.

Moment–curvature relations

The experimental moment curvature relations are compared with the analytical results at the first peak of each drift level in Fig. 21 through 25. Confined and unconfined concrete was modeled using the relations proposed by Saatcioglu and Razvi.[7] Reinforcement stress-strain characteristics were modeled using monotonic relations that closely resembled the experimentally determined relations. For the experimental curves, the moment was taken as applied horizontal load times the height to the point of application above the wall base (150 in.; 3.81 m). The experimental curvature was calculated two ways: 1) as the slope of a best fit line through the strains determined from the LVDTs at the base of the wall; and 2) by dividing the rotation at the first story level by an assumed plastic hinge length of 30 in. (762 mm) or $0.625l_w$. The curvature expected for the design drift level is indicated as ϕ_u on Fig. 21 through 24.

RW3-O—Figure 21 shows that when the column of RW3-O was in tension, the analytical results and experimental results based on the LVDTs are similar. The curvature results computed from the first story rotation are not reasonable; the original data suggests that one of the wire potentiometers may have been sticking in one direction. The slightly lower than predicted ultimate strength at curvatures between 0.0006 and 0.0008 rad/in. (0.024 and 0.031 rad/m) may be due to the onset of buckling in the main longitudinal bars. When the column was in compression (Fig. 22), the experimental curve lies considerably below the analytical curve, and the stiffness degrades rapidly for lateral drift ratios greater than 0.5 percent. The reduction in flexural strength and stiffness under negative loading, compared to positive loading, may be due to shear, or it could be attributed to the effects of cyclic loading. Theses effects include: 1) the reduction in steel stiffness (Bauschinger Effect), and 2) the opening and closing of cracks. The monotonic moment-curvature envelope used in Fig. 22 is unable to account for these effects. Since the column was loaded in tension first, these effects would not show up in Fig. 21. The results from

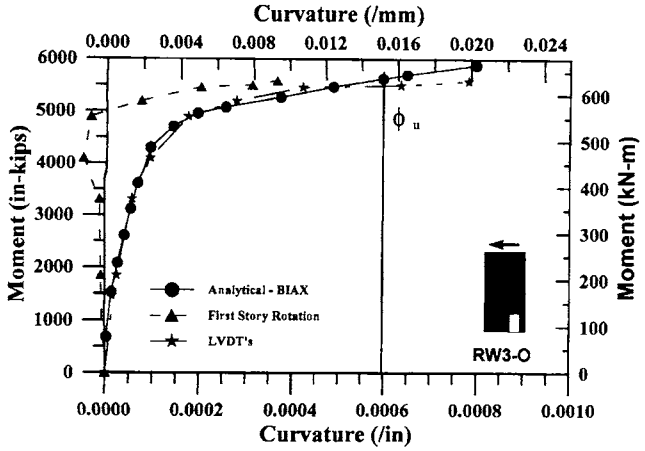

Fig. 21—RW3-O: Analytical vs. experimental moment-curavture response (positive displacement)

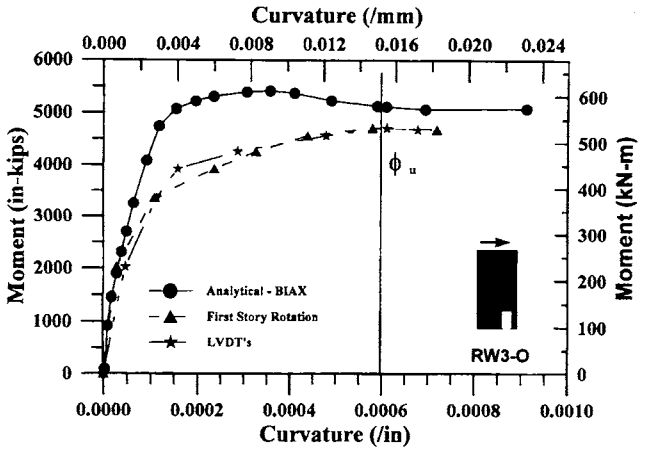

Fig. 22—RW3-O: Analytical vs. experimental moment-curavture response (negative displacement)

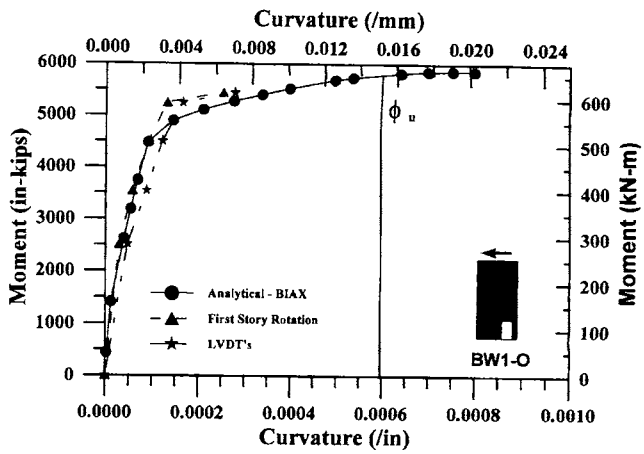

Fig. 23—BW1-O: Analytical vs. experimental moment-curavture response (positive displacement)

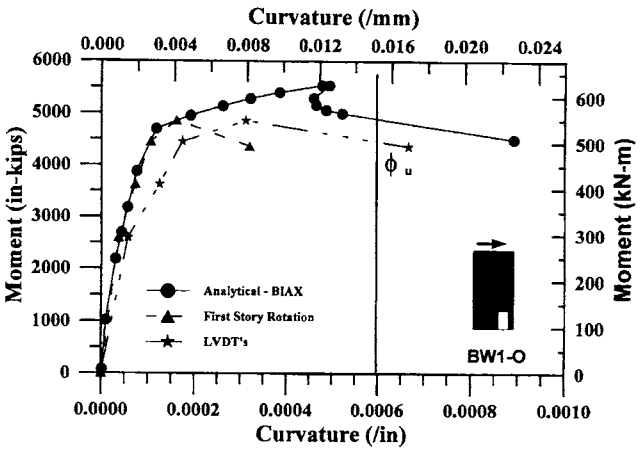

Fig. 24—BW1-O: Analytical vs. experimental moment-curavture response (negative displacement)

the first story rotation seem reasonable for this direction since they are in agreement with the LVDT results, indicating some reliability in the experimentally derived moment-curvature results.

Results for RW2, which did not contain an opening, are presented to assess the influence of the opening and cyclic loading on the experimental determined moment-curvature relations. Moment-curvature relations for Specimen RW2 are presented in Fig. 25 for the first peak of loading in each direction. The plot for RW2 for positive loading (Fig. 25) is similar to that for RW3-O for positive loading (Fig. 21). The initial stiffness and the yield level are quite well predicted, and both experimentally and analytically, substantial deformation capacity is exhibited. The relation plotted for negative loading is quite similar those shown in Fig. 21 and 25; therefore, the cyclic load effects do not appear to have a significant impact of the relations. A slight drop in pre-yield stiffness is observed in Fig. 25 for negative loading. In contrast, the relation for RW3-O for negative loading indicates a much more significant variation in the analytical and experimental relations. Given this evaluation, it is clear that the opening has a significant influence on the moment-curvature response. The main longitudinal tension reinforcement yields at a lower load level then is predicted using the moment-curvature relation (that neglects the influence of shear). However, the deformation capacity of the wall is not impacted, and it is also noted that at the design curvature level the experimental and analytical flexural strengths are very close. In general, use of moment-curvature analysis provides valuable insight into expected wall behavior.

To compensate for the early loss in strength and stiffness of RW3-O compared with the solid wall RW2, it may be appropriate to use additional tensile reinforcement at the north boundary (column in compression). This would compensate for the influence of the compression struts on the tensile force in the boundary longitudinal reinforcement (see Fig. 7). The impact of this additional steel on the concrete compression strains would also have to be evaluated.

BW1-O—The analytical results presented in Fig. 23 and 24 were computed using actual material properties and include the increase in axial load to $0.137A_g f'_c$ from $0.10A_g f'_c$, for which the wall was designed. When the column of Specimen BW1-O was in tension (Fig. 23), the analytical and both experimental curves agree very well up to 1.5 percent drift; however, no data were collected for higher drift ratios due to the deterioration under negative loading. When the

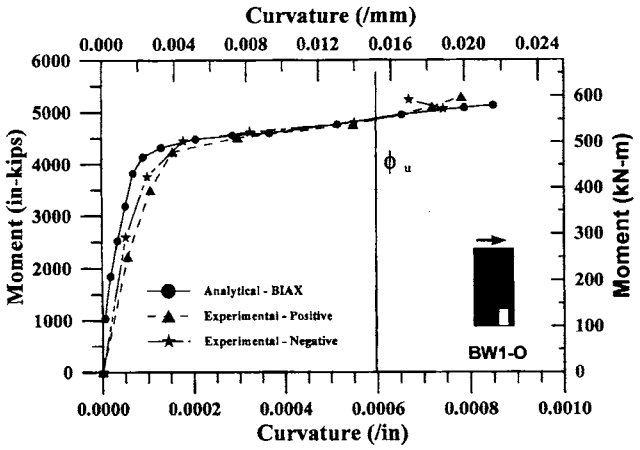

Fig. 25—RW2: Analytical vs. experimental moment-curavture response

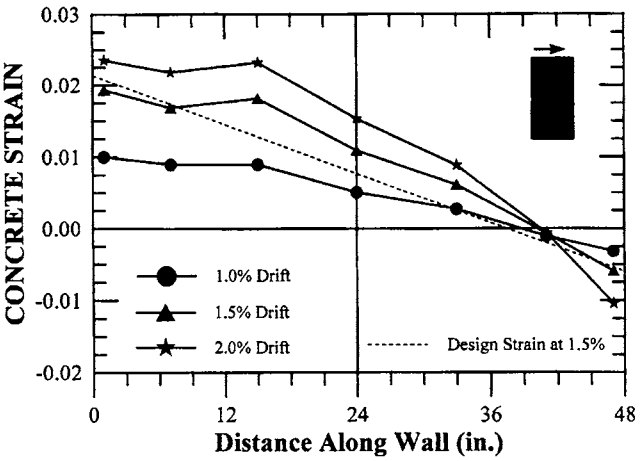

Fig. 26—RW2: Analytical vs. measured concrete strain profiles (positive displacement)

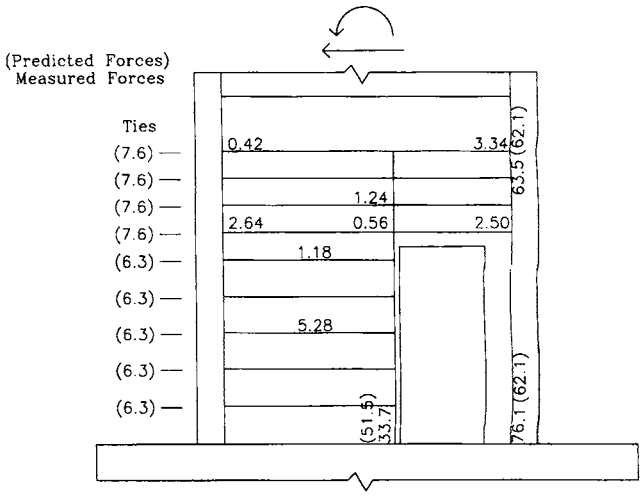

Fig. 27—RW3-O: Predicted and measured bar forces (positive displacement)

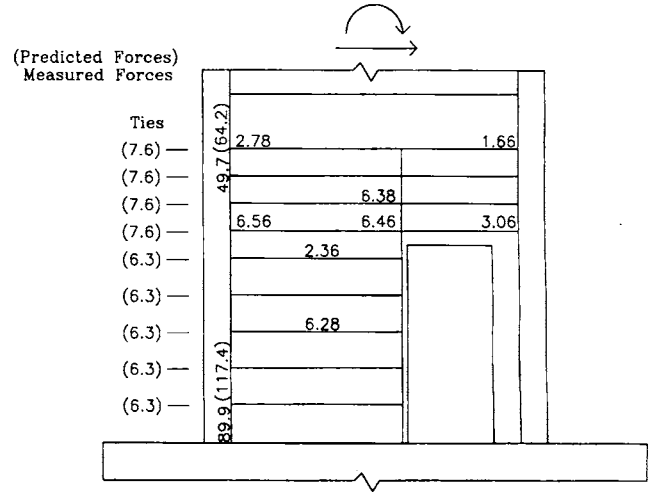

Fig. 28—RW3-O: Predicted and measured bar forces (negative displacement)

column was in compression (Fig. 24), the analytical results predicted the measured response well, up to 1.0 percent drift, beyond which the column began to deteriorate significantly.

The comparison of the moment-curvature relations presented in Fig. 21 through 25 indicates that a monotonic analysis can predict the flexural strength, stiffness, and deformation capacity of slender walls, even when an opening is located in the region of high inelastic deformation. Although there is some discrepancy for the wall with an opening, the overall design philosophy used for the wall design provides a flexible, yet simple, approach for assessing expected behavior.

The results for RW2 and RW3-O (Fig. 22 and 25) indicate that shear forces and deformations effectively reduced the flexural strength of the wall for Specimen RW3-O. Development of simplified analytical techniques to address this behavior are needed. For wall BW1-O, the actual performance was worse than expected due to: 1) a higher axial load was used for the test, $0.137A_g f'_c$, versus the design axial load of $0.10A_g f'_c$; 2) the actual hoop spacing exceeded the specified design spacing in the critical region at the base of the column; and 3) poor behavior of the narrow web section with a single curtain of reinforcement. Although Items 2 and 3 would not be as significant for full scale walls, these items identify areas of design, construction, and inspection that warrant attention.

Strut and tie load paths

This section provides an evaluation of the effectiveness of using the strut and tie modeling technique for design. A comparison is made between the experimental and predicted tensile forces in the vertical and horizontal steel bars in the first story of each wall (Fig. 25 through 28). A reliable evaluation of the compressive forces could not be made since this would involve a complex interaction of the strut angles, the concrete strain and stress, and the steel strain and stress. In Fig. 25 through 28, the predicted forces are shown in parentheses and the predicted tie forces are shown to the left of the figures. In RW3-O, which had two curtains of web steel, the web bar forces indicated are the sum of the forces in the pairs of bars at each location.

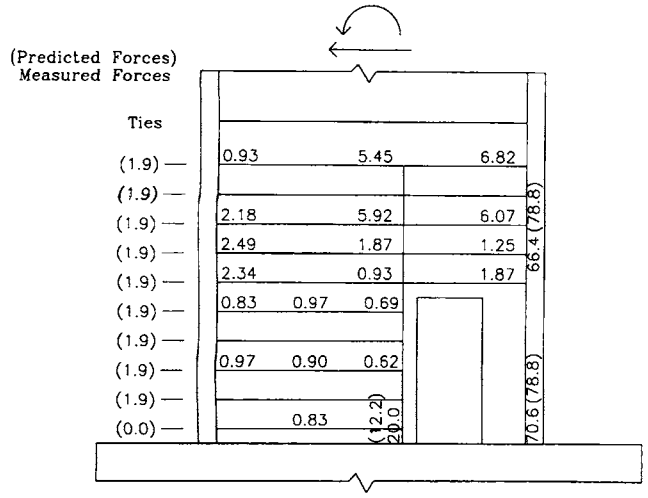

Fig. 29—BW1-O: Predicted and measured bar forces (positive displacement)

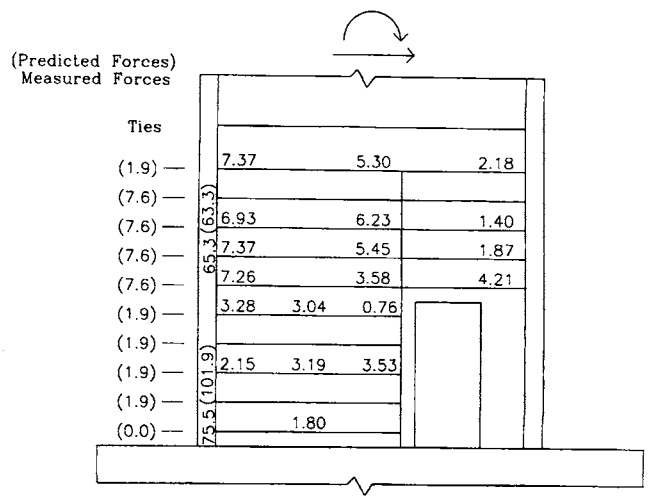

Fig. 30—BW1-O: Predicted and measured bar forces (negative displacement)

The predicted vertical bar forces in these figures were taken directly from the strut and tie models used for the design of the walls (Fig. 7 and 8). The horizontal forces in the model ties were divided among a number of tributary ties in the actual wall. For example, in RW3-O, a single model tie over the opening carries 30.4 kips (135 kN) (Fig. 7). In the real specimen, four pairs of bars were provided at this location resulting in 7.6 kips (33.8 kN) per pair of bars (Fig. 26). The predicted values in the figures were determined using the design horizontal force, neglecting the slight difference in the design forces and the actual applied loads.

The experimental forces were determined from the steel strain gages at 1.5 percent drift for the first peak in each direction of loading. From the strain, the stress was determined from the experimentally obtained monotonic stress-strain relations; therefore, cyclic effects were not considered. The stresses were then multiplied by the area of each bar or pairs of bars to obtain the forces. For simplicity, the forces in the vertical steel were lumped at the boundaries and next to the opening in the figures. Instead of ignoring the contribution of all the vertical web steel, the forces in two web bars were included with each of the vertical forces. For example, in the boundary of RW3-O, the forces in the eight No. 3 (9.5 mm) bars and two pairs of No. 2 (6.4 mm) bars were lumped together. A large difference in the predicted and experimental forces indicates that the loads followed a different path than the one assumed in design.

Finite element modeling[8] has indicated that an increase in either horizontal or vertical web steel alone does not significantly improve the behavior of walls with openings. Also, the strut and tie models developed for the test specimens do not directly indicate a need for vertical web reinforcement. However, as noted previously in this paper, vertical web steel that was provided at the same spacing as the horizontal web steel based on ease of construction compared to diagonal reinforcement and to reduce crack widths. Based on the experimental results, this arrangement was found to be effective.

In all of the comparisons (Fig. 25 through 28), the actual stress in the longitudinal steel was found to be about 75 to 100 percent of the forces predicted by the strut and tie model used for design, indicating that the shear reinforcement selected was used. The forces in the horizontal ties varied somewhat, enforcing the point that the load will follow the stiffest path (since the finer mesh of vertical and horizontal web reinforcement extended above the opening across the entire wall length some redundancy existed). Thus, as long as a reasonable path is provided, the model will provide a suitable, conservative design. Overall, the results indicate that strut and tie modeling provides a good technique for the design of discontinuous regions, where simplified code equations may not apply.

CONCLUSIONS

Experimental results show that, when properly reinforced, slender structural walls with openings at the base can exhibit stable hysteretic behavior and significant ductility, even for the case where the opening is in the flexural compression zone. The large openings at the base did not significantly influence the behavior of the wall compared with results for walls without openings. Vertical cracks over the door opening of RW3-O indicate that the reinforcement at this location was effective in providing a load path around the opening. The following subsections discuss the effectiveness of the following analytical techniques that were used to determine the various reinforcement required for the test specimens: 1) plane sections remain plane and the use of moment-curvature analysis; 2) displacement-based design; and 3) strut and tie modeling and capacity design.

Plane sections and moment-curvature analysis

Evaluation of the strains obtained for the concrete using LVDTs and for the steel using strain gages indicates that, at design drift levels, the strains across the base of the walls had greater deviation from linear than the strains for the solid walls tested by Thomsen and Wallace[5] and Ali and Wight.[2] As well, the strain in the concrete and the steel at a given location were not always the same. The measured strains were sometimes twice those predicted by a sectional analysis assuming plane strains; however, overall moment-curvature response (strength, stiffness, and deformation capacity) was

well predicted for the tested specimens. Although some local variation was observed, the use of a linear strain distribution is reasonable for design of walls in which the relative size of the openings do not exceed those used in these tests.

Displacement-based design

The displacement-based design technique allowed transverse boundary reinforcement to be provided based on the estimated compression strain in the concrete rather than selected based on a nominal stress value. This procedure worked well to ensure that the concrete in the boundary elements had adequate confinement to prevent crushing at high strains. The good agreement between the predicted and experimental moment-curvature relations indicates that displacement-based design is an effective procedure for assessing detailing requirements for transverse reinforcement at wall boundaries. The boundary regions performed well even though the measured compression strains differed somewhat from the strains assumed in the design model.

Strut and tie modeling

Shear was found to play a more significant role in the behavior of walls with openings compared with solid walls. For the specimens with openings, shear contributed approximately 25 percent of the top lateral displacement compared with approximately 10 percent for the solid wall. Strut and tie modeling was effective for the shear design of discontinuous regions, where simplified code equations are not appropriate. Provided a reasonable model is selected, this method will result in a conservative design. Although the strut and tie model did not indicate a need for vertical web reinforcement, a mesh of horizontal and vertical web reinforcement was provided. Test results indicate good inelastic performance with this reinforcement arrangement.

ACKNOWLEDGMENTS

The research in this report was funded in part by the State of New York SUNY Research Foundation and the National Science Foundation through a National Center for Earthquake Engineering Research Grant 92-3112. Additional support was provided by Clarkson University. The assistance of Dr. John H. Thomsen IV with the test setup and data acquisition is greatly appreciated. The opinions, conclusions, and recommendations in this paper are those of the authors, and do not necessarily represent those of the sponsors.

CONVERSION FACTORS

1 in. = 25.4 mm
1 kip = 0.004448 N

NOTATION

A_g = gross cross-sectional area
E_t = steel tangent modulus of elasticity
d_b = longitudinal bar diameter
d_1, d_2 = undeformed length between corners of "X" configuration
d'_1, d'_2 = deformed length between corners of "X" configuration
f'_c = concrete compressive strength
f'_s = stress in compressive steel
f_y = steel yield stress
h = vertical height of "X" configuration to measure shear distortions
h_w = wall height
l = length of "X" configuration to measure shear distortions
l_w = wall length
s = spacing of transverse reinforcing
δ_u = ultimate lateral displacement at top of wall
ϕ_u = ultimate curvature at design drift level of 1.5 percent
γ_{ave} = average shear strain

REFERENCES

1. Wallace, J. W., and Moehle, J. P., "Ductility and Detailing Requirements of Bearing Wall Buildings," *Journal of Structural Engineering*, ASCE, V. 118, No. 6, 1992, pp. 1625-1644.

2. Ali, A., and Wight, J. K., "Reinforced Concrete Structural Walls with Staggered Opening Configurations Under Reversed Cyclic Loading," *Report* No. UMCE 90-05, Department of Civil Engineering, University of Michigan, Ann Arbor, Michigan, Apr. 1990.

3. Wallace, J. W., "New Methodology For Seismic Design of RC Shear Walls," *Journal of Structural Engineering*, ASCE, V. 120, No. 3, 1994.

4. Yanez, F. V.; Park, R.; and Paulay, T., "Seismic Behavior of Reinforced Concrete Structural Walls With Regular and Irregular Openings," *Pacific Conference on Earthquake Engineering*, New Zealand, Nov. 1991.

5. Thomsen IV, J. H., and Wallace, J.,W., "Displacement-Based Design of RC Structural Walls: An Experimental Investigation of Walls with Rectangular And T-Shaped Cross-Sections," *Report* No. CU/CEE-95/06, Department of Civil and Environmental Engineering, Clarkson University, Potsdam, New York, June 1995.

6. Wallace, J. W. , "Seismic Design of RC Structural Walls. Part I: New Code Format," *Journal of Structural Engineering*, V. 121, No. 1, 1995, pp. 75-87.

7. Saatcioglu, M., and Razvi, S. R., "Strength and Ductility of Confined Concrete," *Journal of Structural Engineering*, ASCE, V. 118, No. 6, 1992, pp. 1590-1607.

8. Sittipunt, C., and Wood, S. L., "Influence of Web Reinforcement on the Cyclic Response of Structural Walls," *ACI Structural Journal*, V. 92, No. 6, Nov.-Dec. 1995, pp. 745-756.

9. Taylor, C. P., and Wallace, J. W., "Design of Slender Reinforced Concrete Walls With Openings," *Report* No. CU/CEE-95/13, Department of Civil and Environmental Engineering, Clarkson University, Potsdam, New York, Dec. 1995.